CONF-830640--4

DE83 014036

A HIGH-EFFICIENCY HEAT-PUMP FAN*

T. Wright
R. S. Lackey
S. E. Veyo

Westinghouse Electric Corporation
R&D Center
1310 Beulah Road
Pittsburgh, PA 15235

Prepared under Subcontract 86X-24712C for the
Energy Division
Oak Ridge National Laboratory
Oak Ridge, Tennessee 37830

To be presented to the
American Society of Heating, Refrigerating, and
Air Conditioning Engineers
June 26-29, 1983
Washington, D.C.

*Research sponsored by the Office of Energy Research and Development, U.S. Department of Energy, under contract W-7405-eng-26 with the Union Carbide Corporation.

A HIGH-EFFICIENCY HEAT PUMP FAN*

T. Wright
Nuclear and Process Engineering

R. S. Lackey
Product Design

S. E. Veyo
Heat Transfer and Fluid Dynamics

ABSTRACT

This paper documents efforts toward development of a high-efficiency outdoor air mover for an advanced electric heat pump. The design goal was to halve the outdoor air-moving electrical power. The prototype air mover at 850 rpm delivers 3070 scfm through the prototype outdoor unit with a pressure drop through the coil of 0.09 inches of water and consumes 150 watts of electrical power. The overall air-moving efficiency is estimated at about 35 percent compared with 19 percent for the conventionally-applied heat pump fan. Although this air mover will cost twice as much as the conventional heat pump air mover, this premium cost should be recoverable in less than four years through energy savings. The sound rating (SRN) for this air mover is less than 20. Means for improving fan efficiency by 5 percentage points, motor efficiency by 2.5 points, and to further quiet the fan have been identified.

*Work sponsored by U.S. DOE through contract 86X-2741C administered by the Oak Ridge National Laboratory operated by Union Carbide Corporation.

TABLE OF CONTENTS

A HIGH-EFFICIENCY HEAT PUMP FAN

T. Wright
Nuclear and Process Engineering

R. S. Lackey
Product Design

S. E. Veyo
Heat Transfer and Fluid Dynamics

SECTION 1.0

INTRODUCTION

A 3.5 ton heat pump[1] outdoor air mover is required to move relatively large volumes of air, typically 3000 scfm, through the relatively low flow resistance, typically 0.15 inches of water, due to the heat exchanger and protective grilles.

The outdoor air mover is typically a two-to-four-bladed propeller fan turning at six-pole (1020 rpm) or eight-pole (825 rpm) speed. The propeller blades are of large chord, more or less shovel-shaped, and riveted to a simple steel spider hub driven by the motor. The blades are commonly of constant thickness, perhaps ribbed for stiffness, and of constant camber and incidence and with high solidity, overlapping in some designs. The fan hub is open and air can recirculate in some applications. The propeller rotates in a running ring or shround, many times without curved inlet flare, with a generous clearance of a quarter-inch or more between blade tip and shroud. A restricted fan inlet and a short or nonexistent diffuser ring are commonplace. Consequently, outdoor air mover static efficiencies as applied are generally 20 to 35 percent, rather than the 45 percent peak efficiency indicated in some vendor literature.

The fan motor for residential units is typically a permanent split capacitor type of 1/6 to 1/3 hp rating and of weatherproof design yielding about 55 percent efficiency. With 35 percent fan static efficiency and a 55 percent efficient motor, the overall air-moving efficiency is only 19 percent, and power consumption is on the order of 250 watts. The goal was to halve the outdoor air-moving power.

The preliminary specification for an outdoor air mover called for an air delivery of 2900 scfm against an upstream flow resistance of 0.20 inches of water with a static efficiency of 60 percent. (The unit pressure drop with a dry coil was anticipated to be about 0.10 inches of water. In order to ensure adequate airflow under heavy frosting conditions the fan pressure rise requirement was specified as double the nominal dry coil pressure drop.) The motor was required to be at least 65 percent efficient. Air-mover size was constrained to 24 inches in diameter and 12 inches in height, exclusive of mounting flanges. The fan noise was not to exceed a noise rating (SRN) of 20, and a rating of 18 or less was desired[2].

Since a quiet fan with good static efficiency was required, a multivane, axial flow design was proposed. A fan of this type has five or more blades of relatively narrow chord and low solidity. A large solid hub is used to prevent recirculation.

SECTION 2.0

TECHNICAL DISCUSSION

2.1 BACKGROUND

Selection of a fan for the outdoor unit of a heat pump involves several considerations, including air volume flow, air static pressure, sound levels, packaging, fan motor characteristics, and cost. The traditional method for characterizing the operating regime of fans is specific speed, a parameter relating rpm, the delivered volume flow rate, and the static pressure rise across the fan. Both dimensionless and dimensional forms of this parameter are in common use, but all use the same exponents to modulate the volume flow and pressure rise[3].

Two measures of air-mover efficiency are in use, total efficiency and static efficiency. Total efficiency is a ratio calculated as the total power imparted to the moving air stream divided by the shaft power absorbed by the air mover. The total power in the air stream, the air horsepower, consists of a static effect or change in potential energy due to the static pressure rise imparted by the air mover, plus a dynamic effect due to kinetic energy change in the flowing air across the air mover. The kinetic energy of the moving air stream is of no value to ventilating machinery, so the static efficiency is the more meaningful measure of air-mover efficiency. Static efficiency is defined as the ratio calculated from the static pressure head imparted to the air stream by the air mover divided by the shaft power, per unit of mass flow, absorbed by the air mover, with all quantities expressed in consistent units.

The outdoor unit of a heat pump typically requires a high air-volume flow at a low static head; it is therefore a high specific speed application.

A propeller fan is clearly best suited for this application, and most heat pump outdoor units do use propeller fans.

Space limitations generally result in a restricted fan inlet and short diffuser rings. Product cost pressure has substituted high air flow for heat exchanger surface and forced a tradeoff of low air mover cost for good aerodynamic design. Consequently, outdoor air mover static efficiencies as applied are generally 20 to 35 percent rather than the peak efficiency near 45 percent as might be expected. With a 35 percent fan static efficiency and a 55 percent efficienct fan motor, the air-moving efficiency is only 19 percent. In a representative 4-ton unit the outdoor fan motor draws about 250 watts, less than 5 percent of the system power input at 47°F and about 8 percent at -20°F. Obviously, increasing the fan/motor efficiency will not dramatically increase the seasonal coefficient of performance, but the cost of the electricity used to drive the outdoor fan is not insignificant. A 250-watt motor operating for 6000 hours per year will have an annual energy cost of $75 at an electricity cost of 5¢/kWh. The potential savings of $30/yr is sufficient to warrant consideration of more expensive fans and fan motors.

A typical propeller fan used in HVAC systems is a four-blade design with blades stamped from aluminum sheet and riveted to a steel "spider" hub. The blades are commonly of constant thickness, camber, and incidence, and of high solidity, overlapping in many designs. The leading and trailing edges of the blades have sharp corners, resulting from the stamping process. The hub of the fan wheel is relatively open; air can recirculate through the hub in some applications.

Alternate fan designs which will provide good static efficiency over a wide range of operating speeds are available. A multivane axial flow design is well suited for this application. A fan of this type has five or more blades of relatively narrow chord and low solidity. A large solid hub is used to prevent recirculation.

The objective for outdoor fan improvement was to halve the air-moving watts by raising fan static efficiency to the 60 percent range while employing a high-efficiency motor (65 percent efficiency) to drive the fan.

The requirements and specifications for the outdoor fan assembly were formalized as follows. The fan should be a vertical shaft-type directly driven by the motor. It should draw air through the outdoor heat exchanger and deliver 2900 cfm against an upstream static pressure resistance of 0.2 inches of water. The fan should operate stably at 80 percent of design flow (2320 cfm) and should achieve a static efficiency approaching 60 percent. Size is constrained to a 24-inch maximum outside diameter with a desired overall length of 12 inches or less. Noise (according to ARI Standard 270-75)[2] should not exceed a noise rating of 20, and 18 was desired.

2.2 AERODYNAMIC ANALYSIS AND BREADBOARD FAN DESIGN

The design procedure applied to the heat pump outdoor fan had three levels. First, since a quiet fan with good static efficiency was desired, the performance and size constraints were examined to produce a fan having minimal blade surface velocities[4]. Second, since high static efficiency was the primary design criterion, the fan parameters developed in the first level were examined in greater detail with systematic variation of the parameters, using an approximate efficiency analysis procedure[5]. Third, the best design candidates developed in the second level were examined in detail using the more rigorous computerized analyses (proprietary programs). Brief descriptions of these analyses and the resulting designs follow.

As used in the first level of analysis, an aerodynamic parameter was developed[4] to relate subsonic axial fan noise to the fundamental flow behavior in the blade row of an axial fan. This variable is the peak

blade surface velocity which, in an axial fan, is dependent on local relative velocities and the induced blade surface velocity associated with the generation of the head, H. The Euler equation[3] is used to determine blade circulation, and the Kutta-Joukowski theorem[6] to relate circulation to induced surface velocity. Induced velocity with the blade relative velocity yields the ideal blade surface velocity. For conditions which are not ideal, surface velocity will not be uniform and induced velocity will be amplified to account for losses. Defining pressure rise coefficient Ψ_T and flow coefficient ϕ as

$$\Psi_T = 2gH/V_T^2$$

$$\phi = V_a/V_T \quad , \tag{2-1}$$

here V_T is tip speed and V_a is the axial velocity component. Using K to represent the relative magnitude of a velocity peak or spike on the blade along with η_T as total efficiency, yields the blade surface peak velocity according to

$$V_p = K\, V_T\, ((x^2 + \phi^2)^{\frac{1}{2}} + \Psi_T/(4\sigma \times \eta_T)) \quad . \tag{2-2}$$

σ is local blade solidity. $\sigma = C/s$ where C and s are blade chord and circumferential gap. This is the parameter which is minimized in the first level design sweep. As seen from Equation (2-2), V_p is a function of diameter and rotating speed (through V_T), hub size (through ϕ), blade parameters (through σ and x), pressure rise through Ψ_T, and efficiency. An initial prediction of noise level, for a fan with outlet guide vanes, can be calculated from

$$PWL = 50.9 \log_{10} V_p - 28.1 \tag{2-3}$$

where PWL is overall sound power in dB re 10^{-12} watts. V_p is in ft/sec units.

An example of peak velocity analysis is given in Figure 2-1. Calculated peak blade surface velocities are shown for direct-connected speeds of 1725, 1135, 840, and 665 rpm. Diameter was varied from 1 to 3 feet, and the noise prediction associated with the diameters for which V_p is a minimum are indicated in the figure. (Also shown are noise values at diameters associated with best static efficiency performance). This result indicates that the fan should be designed with the lowest acceptable motor speed and a reasonably large diameter, although the size constraint of $D \leq 2$ ft is acceptable in terms of minimum velocity.

The second level of analysis, estimation of static efficiency, is carried out in the range of sizes and speeds which are near the minima shown on the curves of Figure 2-1. Estimation is based on an approximate method developed to model the dominant loss modes of axial fans and includes the influence of swirl or vane row loss, blade profile loss, tip clearance loss, losses in a downstream diffuser, and velocity pressure loss at the discharge of the fan[5]. Total efficiency is estimated according to

$$\eta_T = (1 - K_\ell)\, C_{p_o} / (C_{p_o} + C_{p_d} + C_{p_{TL}}) \quad . \qquad (2\text{-}4)$$

Here, K_ℓ represents an estimate of total pressure lost in the vane row and diffuser. The power coefficients (C_p's) are defined as follows:

$$C_{p_o} = \phi\, \psi_T$$

$$C_{p_d} = .03\, \bar{\sigma}\, (0.2 + 0.33\, \phi^2)/(1 + 1.78\, \phi^2)^{\frac{1}{2}} \qquad (2\text{-}5)$$

$$C_{p_{TL}} = 0.158\, K_s\, \sigma_T$$

where ϕ and ψ_T are defined in Equation (2-1), $\bar{\sigma}$ is mean blade solidity (σ at $x \approx .75$), σ_T is blade solidity at the blade tip, and K_s is given by

Curve 760510A

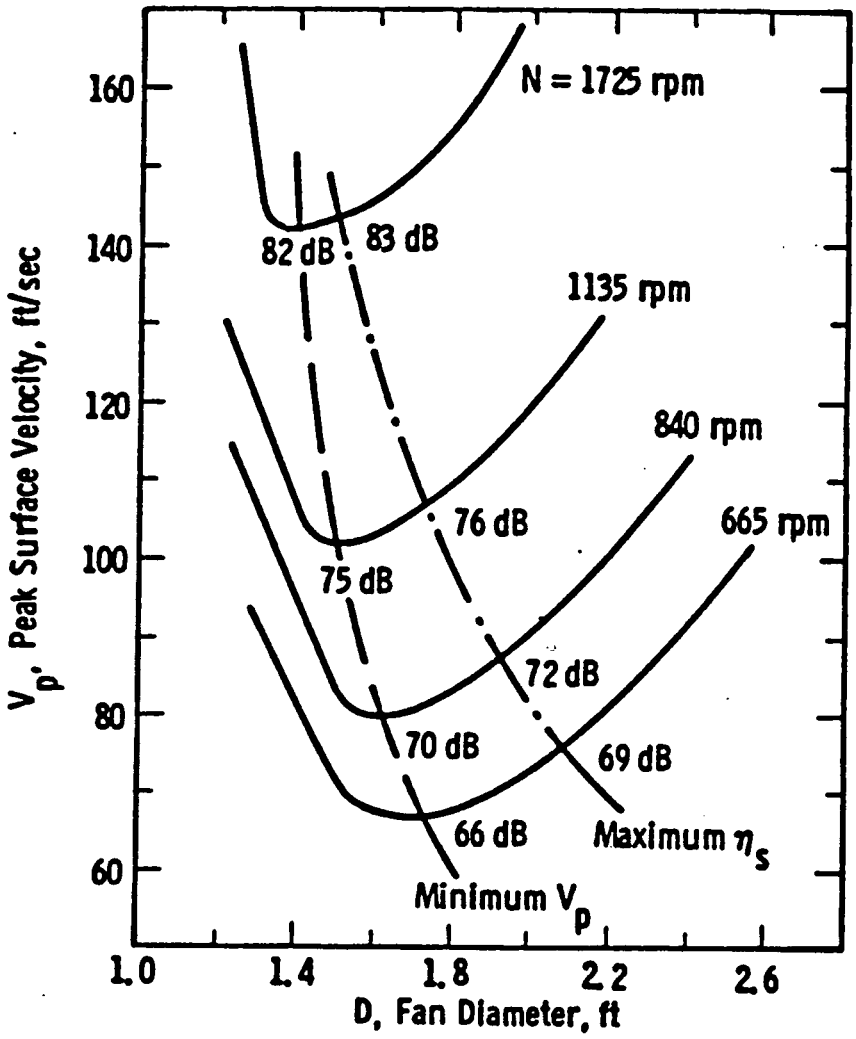

Figure 2-1. Blade Peak Surface Velocity (Noise in dB re 10^{-12} Watts).

$$K_s \approx 0.20 \tanh (20\ \delta_T) \qquad (2\text{-}6)$$

where δ_T is the blade tip gap defined as

$$\delta_T = 2G/D \quad . \qquad (2\text{-}7)$$

An example of the second sweep efficiency analysis is shown in Figure 2-2. Calculated efficiencies are shown for the four speeds and diameter ranges used in the peak velocity studies. Here, K_ℓ was estimated by using a nominal vane loss and restricting diffuser length to 1 ft. Blade tip clearance was set at 1/8 inch. Static efficiency is calculated directly from total efficiency through use of the diffuser velocity pressure loss based on the ratio of length-to-inlet annulus height with maximum allowable recovery or expansion[7]. Static efficiency is defined as:

$$\eta_s = 1.576 \times 10^{-2}\ \Delta P_s\ Q/W_s \qquad (2\text{-}8)$$

where

ΔP_s = static pressure rise across fan (inches of water)

Q = volume flow rate (cfm)

W_s = fan shaft horsepower (hp)

η_s = static efficiency (%).

As seen in Figure 2-2, the peak static efficiencies at different speeds correspond to slightly larger diameters than those for minimum velocity. Noise predictions, shown in Figure 2-1, indicate that a modest increase is incurred by moving from the minimum velocity point to the point of best static efficiency. Since the lowest allowable motor speed was set at 840 rpm, these results indicate that the best fan design for the application and constraints has a diameter of 2 feet running at 840 rpm and should produce a maximum static efficiency in the range of 55 percent. More thorough studies, including limitations on blade row diffusion and

Curve 760511A

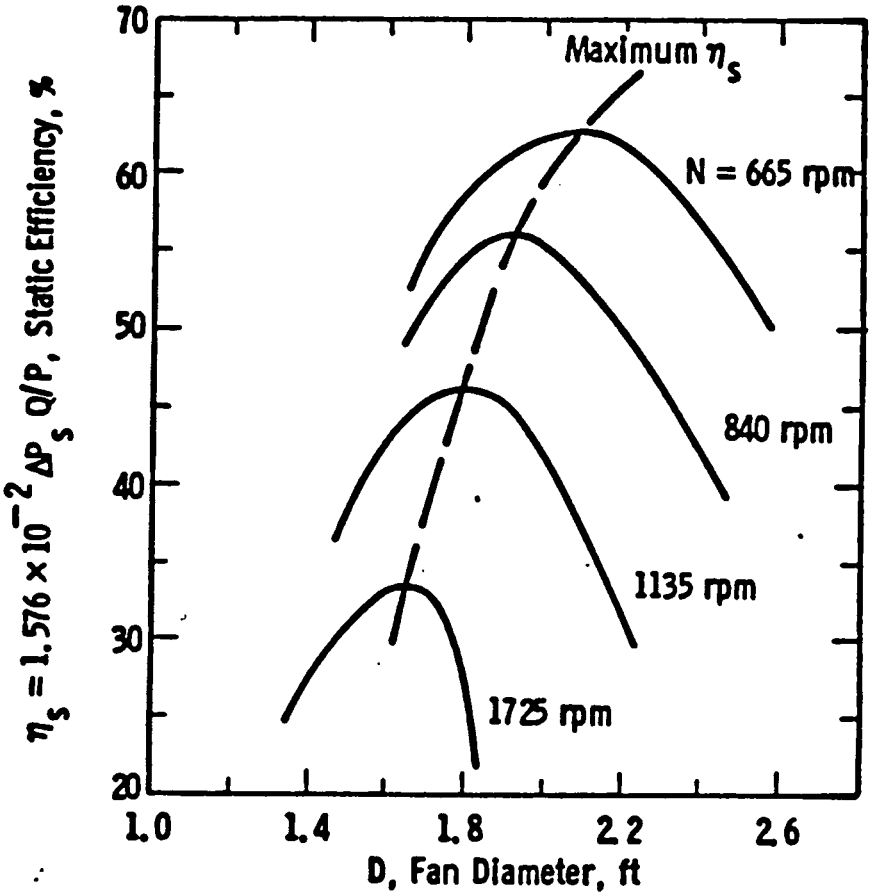

Figure 2-2. Constrained Optimization of Static Efficiency at Direct-Connected Fan Speeds.

a more careful treatment of vane row and diffuser set the hub diameter at 1 foot and indicated the need for high vane row solidity.

The sized fan parameters from the second level design sweep were then used to initiate more detailed design studies, incorporating a more rigorous axial fan analysis computer code.

This code is a design analysis computer program which provides a complete geometric description of an axial flow turbomachine, based on input requirements in terms of head rise, volume flow rate, rotational speed, and diameter. The solution or design procedure is based on three basic elements--an inviscid, incompressible streamline solution; a semi-empirical cascade lift-prediction model; and an empirical loss and loading-limit calculation.

The inviscid solution for the flow through a blade or vane row is governed by the Euler equation with conservation of mass and determination of energy addition associated with total head rise through the machine. This flow is constrained to satisfy "simple" radial equalibrium and radial velocities as such are not considered[3].

Blading parameters are chosen at each radial station of the turbomachine which will generate the required flow patterns. Blade parameter selection is based on the theoretical work of Mellor[8]. Mellor's solution has been empirically modified for this work based on correlations with extensive NACA 65-series airfoil cascade data[9].

To augment and control the use of the cascade calculation, a method was developed to estimate the losses associated with a given blade or vane in a two-dimensional cascade and a correlation was developed to provide a conservative estimate of the maximum load a blade can support without suffering severe energy losses. Loading limit is provided by a correlation of the permissible range of blade angle of attack about the

design or minimum loss value and relates this range to the cascade parameters[9]. Both correlations yield conservative results and serve primarily to eliminate poor design choices and to limit ranges of investigations.

The basic framework of this code has been extended to include more rigorously the effect of tip clearance on both tip losses, annular flow blockage[10], and the onset of stall associated with end wall flow separation or reversal[11]. In addition, the onset and development of rotating stall and re-entry of the fan performance curve from this condition are included, based on the concepts of stall cell behavior[12].

The design code was supplied with running speed, diameter, approximate hub diameter, and blade solidity limits, along with estimated diffuser losses[7] and the performance requirements. Extensive and systematic variation of the detailed design parameters was carried out in order to optimize the static efficiency. Resulting blade and vane row parameters are tabulated in Tables 2-1 and 2-2. Static efficiency predicted by the analysis was 57.9 percent. This result is in substantial agreement with the earlier more approximate calculation (55 percent).

2.3 BREADBOARD FAN TEST RESULTS

The test stand with instrumentation is shown schematically in Figure 2-3. Torque is measured on the strain-gauge-instrumented reaction beam of the cradle-type dynamometer, and speed is read on a digital readout pulse counter operating from a 60-tooth gear. These data, along with static load calibration and rotating tare readings, provide horsepower determination. Pressure drop across the nozzle plane measured on a calibrated electrical strain gauge pressure transducer and static pressure measured at the fan discharge plane provide the flow-pressure rise performance data. All data handling and reduction, including scaling of performance to standard air density and reference fan speed, are done according to AMCA/ASHRAE standards[13].

Dwg. 7765A23

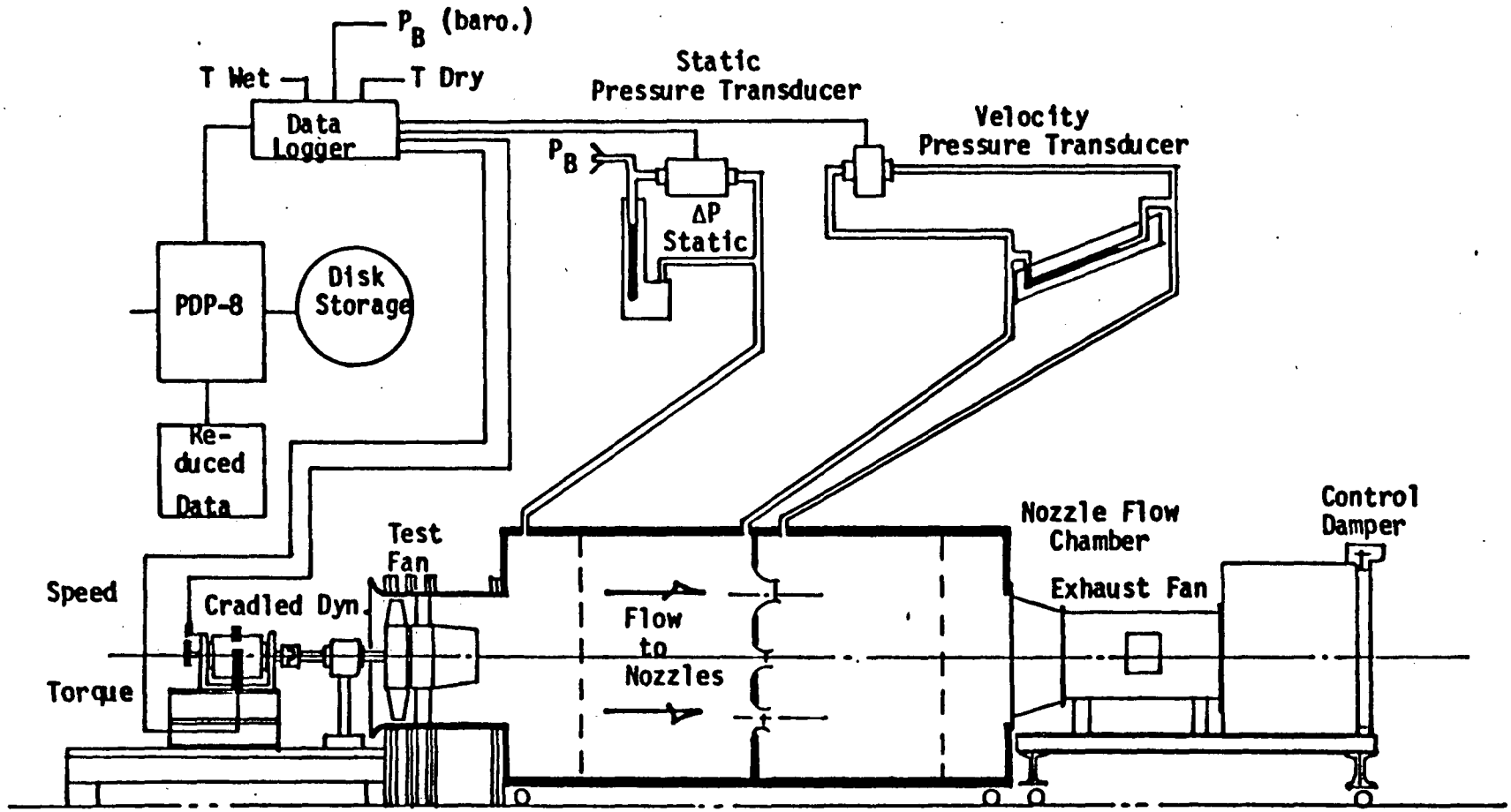

Figure 2-3. Schematic Arrangement of Instrumentation and Test Stand.

TABLE 2-1

BREADBOARD FAN BLADE DESIGN PARAMETERS

x Location (-)	σ Solidity (-)	ϕ_c Camber (degrees)	α_g Pitch (degrees)
.50	0.800	18.85	34.02
.55	0.727	16.11	30.76
.60	0.666	14.06	28.09
.65	0.615	12.34	25.83
.70	0.571	11.06	23.94
.75	0.535	9.92	22.29
.80	0.500	9.04	20.86
.85	0.470	8.40	19.53
.90	0.444	7.73	18.42
.95	0.421	7.00	17.49
1.00	0.400	6.48	16.59

Note: 8 blades unequally spaced

Blade	Angle (degree)
1	35.6
2	90.0
3	144.4
4	180.0
5	215.6
6	270.0
7	324.4
8	360.0

TABLE 2

BREADBOARD VANE DESIGN PARAMETERS

x Location (-)	σ Solidity (-)	ϕ_c Camber (degrees)	α_g Pitch (degrees)
.50	3.00	35.0	75.0
.55	2.73	32.8	77.2
.60	2.50	31.1	78.5
.65	2.31	29.7	79.7
.70	2.14	28.0	80.7
.75	2.00	27.5	81.5
.80	1.88	26.8	81.1
.85	1.77	26.1	81.7
.90	1.67	25.6	82.2
.95	1.58	25.3	83.6
1.00	1.50	25.0	84.0

Note: 31 vanes equally spaced, with constant 3.65-inch chord

A breadboard axial fan was fabricated with an acrylic hub, acrylic blades and vanes, with a fiberglass inlet flare/running ring and a sheet metal diffuser. The blades consist of hot-formed 1/8-inch-thick sheet material mounted on steel tangs to provide adjustable pitch capability. The stator vanes were also hot-formed from 1/8-inch-thick sheet material and were glued into an annular section consisting of a 12-inch-od inner cylinder and a 24-inch-id ring, both 4 inches long and of acrylic. The diffuser section was formed with a 24-inch-id sheet metal cylinder and a conical sheet metal inner body mounted to the center section of the vane row. Both a 12-inch and a 6-inch diffuser were tested. A photograph of the assembly, as prepared for a breadboard fan test, is shown in Figure 2-4. Final test results for the air mover with 6-inch diffuser are summarized in Figure 2-5. The configuration for this test included all components of the fan: inlet flare, blade row, vane row, and 6-inch diffuser.

The performance curves for the outdoor fan (Figure 2-5) show that pressure rise and flow rate intersect the system resistance curve (based on 2900 cfm at 0.2 inches of water) slightly above the design target. Static efficiency for this operating condition is 52 percent with a shaft power requirement of 0.185 hp. The characteristic curve for the fan is very smooth with no regions of positive or unstable slope. At 80 percent of design flow (2320 cfm), the fan operates stably and smoothly. At flows of less than 80 percent of design, the fan continues to operate in a stable manner, with usable flow-pressure performance, although very significant increases in required power and generated noise accompany performance in this flow range. The mechanism for this unusually stable axial fan performance is the pattern of the blade stall occurrence. As flow is decreased below about 2300 cfm by throttling, the outer one-third of the blades enters into a stable part span stall-cell operating mode[12] with strong flow reversal at the tips and forward flow just inboard. On the inner two-thirds of the blade the flow patterns appear to be perfectly normal with clean, strong axial flow through the fan. This pattern of

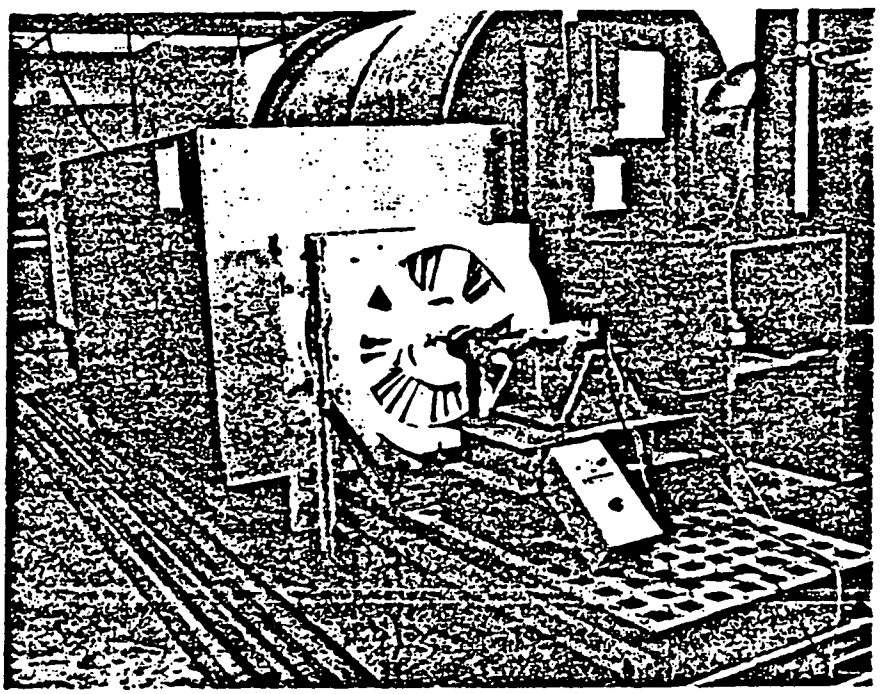

Figure 2-4. The Breadboard Outdoor Fan Assembly Installed on the Test Stand.

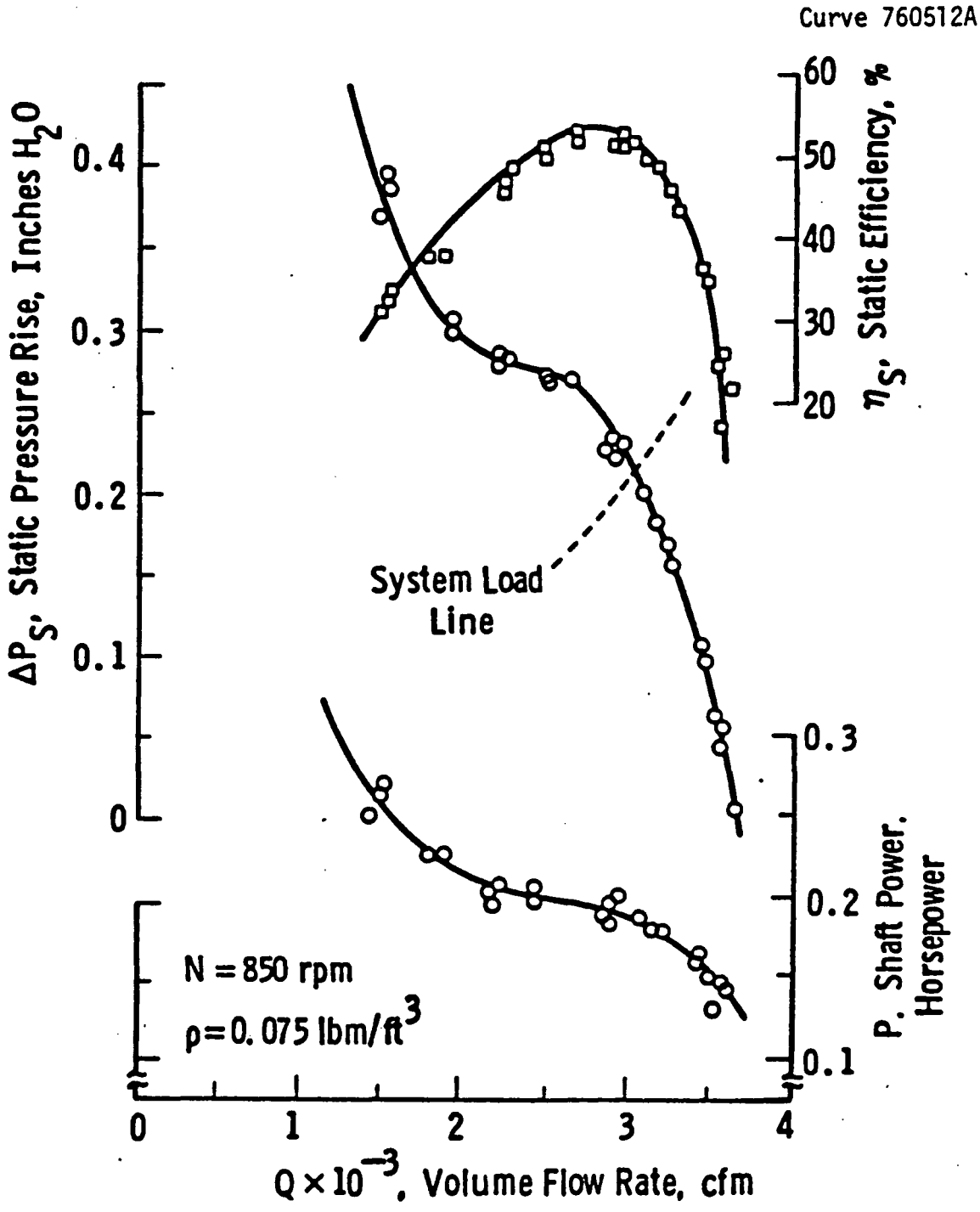

Figure 2-5. Breadboard Outdoor Fan Performance (6-Inch Diffuser, pitch angle α_{g_R} = 33.8°)

partial through-flow persists at least down to 1000 cfm flow delivery at about 0.5 inches of water.

The breadboard fan assembly was tested extensively on the fan test stand shown in Figure 2-3. For blade pitch angles ranging from 31 to 41 degrees, performance was measured with the full assembly, with the rotor only, and with and without the vane row and diffuser installed. Figure 2-6 provides a sample of these results, and the relative value or contribution to efficiency of the various components can be seen.

Because the breadboard fan was tested on a plenum chamber requiring an exhauster fan to overcome the pressure drop across the flow-measuring nozzles, it was not possible to perform meaningful noise measurements. However, approximate dBA meter readings with the fan detached from the flow box (running at free delivery) and subjective listening indicated that the fan was very quiet with no perceivable tonal content in the noise spectrum.

2.4 PREPROTOTYPE FAN

The breadboard fan achieved a static efficiency of 52 percent when delivering 3000 scfm with a pressure rise of 0.21 inches of water through the specified outdoor unit resistance (0.2 inches of water at 2900 scfm). The fan required 0.185 shaft horsepower. This performance was acceptable for the preprototype system, but the anticipated cost of an air mover replete with high solidity stator vane row was judged to be unacceptable.

In order to reduce the cost of the air mover, the stator vane row was removed from consideration. It was expected that this would penalize static efficiency by about 5 percent and thereby raise the shaft power requirements to 0.195 horsepower, based on testing with various combinations of components of the breadboard fan assembly.

Curve 760513A

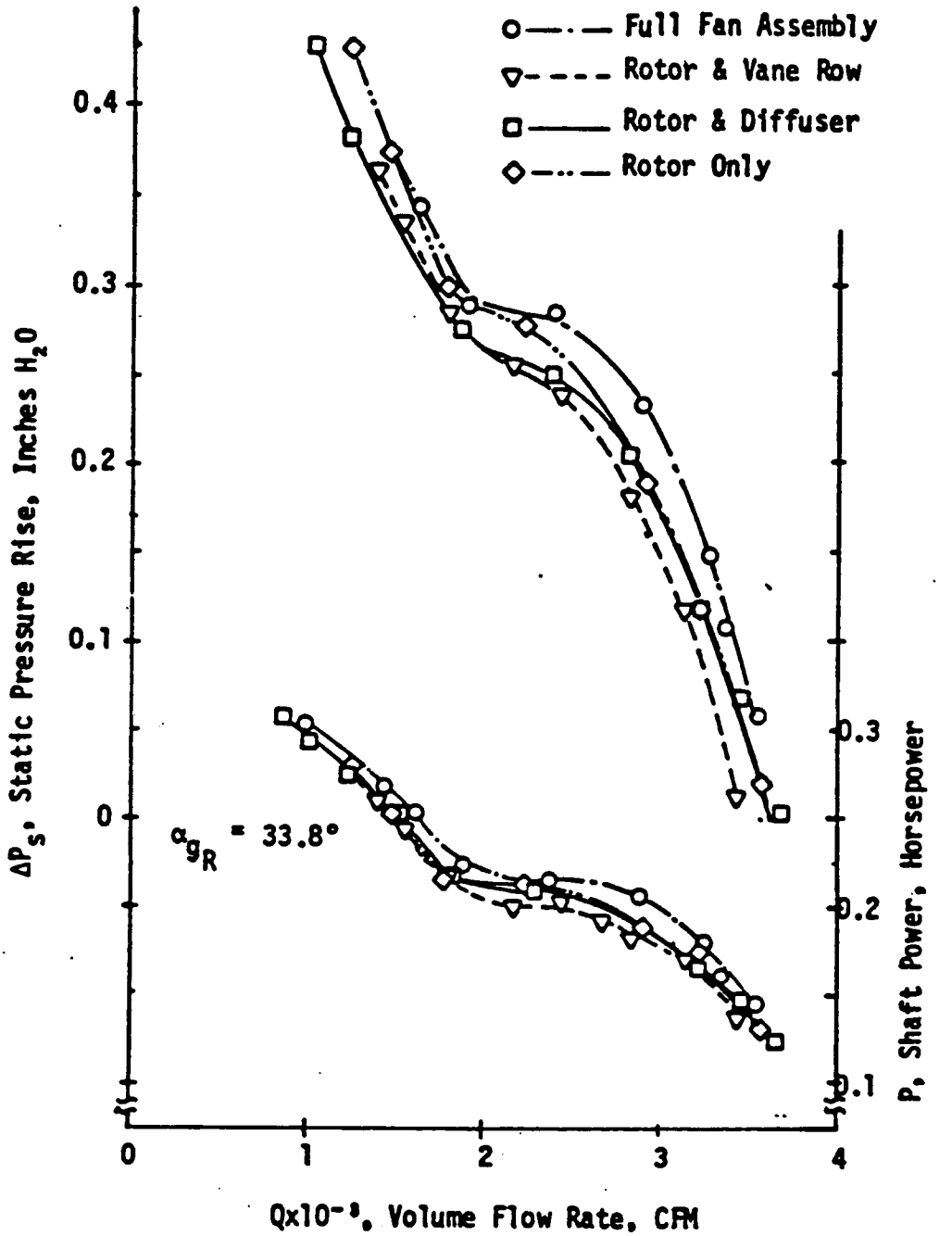

Figure 2-6. Composite Performance Curves for the Outdoor Fan Model with 33.8-Degree Blade Pitch Setting. N = 850 RPM, ρ = 0.075 lb/ft^3.

Rather poor performance observed for the annular diffuser with a cylindrical outer wall and inwardly-tapered inner wall led us to consider a relaxation in the specification for a 24-inch maximum diameter in order to incorporate an outwardly-expanding outer wall for the diffuser. As revised, this specification called for a 27-inch maximum diameter at the exit of the diffuser. (Note that this corresponds with the diameter of the recommended inlet flare.) In order to achieve adequate diffusion, an inner wall was specified with 7-degree taper. The performance curves of Figure 2-6 (for rotor-only) were used, along with estimates of diffuser velocity pressure recovery[7] to estimate the performance of this preprototype fan. Recovery of blade-row annulus velocity pressure was estimated at 35 percent.

The propeller blade specifications were unchanged since the conical diffuser was expected to largely compensate for the removal of the vane row. A completely molded propeller from plastic was considered highly desirable, but project resources would not permit purchase of the necessary tooling. A fabricated assembly consisting of aluminum sheet blades clamped in a two-piece clamshell hub was designed as the best alternative. The fan blade was cut from 2024 aluminum sheet, .060 inch thick, annealed, formed in expedient tooling, and then precipitation-hardened to T4 temper. Two hubs were machined, one from aluminum and one from Noryl® plastic. The production design is envisioned to use a precision die molded plastic hub and blade clamp.

The fan hub is mounted to the motor shaft via a hub insert and the motor suspended shaft down in the shroud by a wire form bellyband carrier motor support. This subassembly is shown in Figure 2-7. The shroud uses the 2-inch radius inlet flare recommended by the breadboard fan analysis.

In order to cool the motor, air flow through the motor housing, the tapered inner wall of the diffuser, must be ensured. An overhung lid with an annular gap was tried, but found inadequate. Inasmuch as the

wire form protective grille at the discharge has a center cover disk, a hole was placed in the center of the motor housing end cap. Since this hole is in a region with higher static pressure than the gap between fan hub and the diffuser center body, the fan will pump air out of the annular gap between hub and diffuser center body, with supply air entering through the hole in the motor center body end cap, the annular gap at the periphery of the center body at discharge, and through the clearance openings for the wire form motor support. The general appearance of this sheet metal diffuser center body/motor cover is not very satisfying, but resources did not permit further design refinement.

2.5 FAN MOTOR

The specifications developed for the outdoor fan motor were designed to yield high reliability as well as high efficiency. These specifications are as follows: The heat pump outdoor fan motor is to be a permanent split capacitor type with 8 poles, totally enclosed and nonventilated with cooling provided by flowing air over the exterior. Power is to be 230/208 volt, 60 Hz, single phase. Direction is to be reversible by external reconnection. The operational environment is to extend from -20°F to +130°F. The expected life is to be 50,000 hours. The bearing system is to be double sealed ball bearings with synthetic grease (Mobil 28). Auxiliary winding insulation is to be Westinghouse Omega-Klad-EK; main winding insulation is to be Westinghouse Omega-Slip-HA; varnish is to be double dip polyester. Frame length is to be extra long (5.5 inches maximum) and the end bell is to be sealed with silicone RTV. Independent thermal protection is to be provided with the leads for main and auxiliary windings and the thermal cut out to be brought out of the frame. Leads are to be 24 inches long and potted in insulation tubes with a sealing grommet. Mounting is to be with shaft vertical and down. Design output is to be 0.20 horsepower at 825 rpm and 65 percent efficiency.

The 0.2 hp, 8-pole fan motor design employs a 2.47-inch stack with an approximate balance between the weight of copper in the main and auxiliary windings. The turn ratio (effective auxiliary turns to effective main turns) is 1.318. The capacitor required for this motor is 4 μfd. The motor has a medium resistance rotor which, on a horsepower per unit basis, is 0.0654 per unit resistance. One feature of the design effort

was an attempt to effect the maximum feasible utilization of the slots within manufacturing capabilities and to run at rated power close to balanced operation.

If a low resistance rotor were to be substituted, the efficiency at full load should improve to 67.5 percent.

2.6 PREPROTOTYPE OUTDOOR AIR MOVER PERFORMANCE

Project resources did not permit the preprototype outdoor air mover to be tested in the test cell of Figure 2-3. The first preprototype air mover was instead installed in the preprototype outdoor unit and tested in the heat pump test facility as part of an operating system. As tested, it delivers 3070 scfm through the outdoor unit at 850 rpm with an upstream (suction side, coil only) pressure drop of 0.09 inches of water with a dry coil. The fan motor consumes 150 watts of electrical power. In low-speed operation, the air mover rotates at 609 rpm and consumes 78 watts of electrical power. Estimated performance for the unit, based on Figure 2-6 and 35 percent recovery of annulus velocity pressure, was 3070 scfm with overall pressure rise of 0.16 inches of water. Shaft power was estimated at about 120 watts.

The second preprototype outdoor unit was tested in the acoustic laboratory reverbatory room for radiated noise. Since the outdoor unit was not coupled to the heat pump control system, noise measurements were obtained for slightly different rpms than protoypical. Noise data are listed in Table 3 for a fan speed of 860 rpm. The SRN of the preprototype fan is less than 20. Note that the diffuser walls have not received any acoustic noise treatment. Note also that the wire form grille was fabricated from rather thin gauge wire. In prototype form a more substantial grille is recommended, since the one used tended to vibrate excessively. The addition of an acoustical noise-absorbing material to the diffuser and running ring plus a more substantial grille would lower the SRN.

TABLE 2-4

NOISE AT 860 RPM

Band No.	Frequency Hz	Sample PWL	Discrete Adjustment	Rating Index
20	100	79.0	0.0	1.7
21	125	79.9	-0.5	2.0
22	160	77.4	0.0	2.0
23	200	77.3	0.0	2.4
24	250	75.2	0.0	2.3
25	315	76.6	0.0	2.8
26	400	76.2	0.0	3.0
27	500	74.9	0.0	2.8
28	630	73.8	0.0	2.6
29	800	73.8	2.5	3.0
30	1000	69.9	0.0	2.0
31	1250	70.1	0.0	2.3
32	1600	68.9	0.0	2.8
33	2000	67.7	0.0	3.2
34	2500	66.0	0.0	3.2
35	3150	64.4	0.0	3.0
36	4000	62.3	0.0	2.6
37	5000	58.7	0.0	1.9
38	6300	55.5	0.0	1.4
39	8000	53.3	0.0	0.6
40	10000	51.3	0.0	0.2

ARI sound rating number: 20. (19.755)

SECTION 3.0

SUMMARY

The outdoor air mover as developed for the preprototype advanced electric heat pump is shown in Figure 3-1. In order to approach our performance goal, at reasonable cost, it was necessary to relax the constraint upon subassembly diameter of 24 inches. As shown, the conical, outwardly-expanding diffuser shroud exit diameter is 27 inches, with the overall diameter of the mounting flange being 31 inches. The overall height of this subassembly is 12 inches and the radius of the 90-degree inlet flange is 2 inches. The propeller, as shown in Figure 3-2, is 24 inches in diameter with a hub-to-tip ratio of 0.5. A conical cover for the motor extends inward from the hub diameter to provide the inner wall of the annular-shaped, 6-inch-high diffuser. The eight propeller blades of constant chord extend nonuniformly spaced from a clamshell hub. The blade spacing pattern has two planes of symmetry. The blades are fabricated from uniform thickness .060-inch aluminum (2024) sheet, cambered and twisted. Two propellers have been fabricated, one with a machined plastic hub and the other with an aluminum hub.

Matched to a two-speed, high-efficiency drive motor, this air mover delivers 3070 scfm of 47°F air through the preprototype outdoor unit with an upstream or suction side static pressure drop of 0.09 inches of water at 850 rpm. The fan motor consumes 150 watts of electrical power. Estimated static efficiency is 50 percent. In low-speed operation, the air mover rotates at 609 rpm and the motor consumes 78 watts of electrical power.

The factory cost of this air mover subassembly, consisting of shroud, motor cover, motor support, motor, discharge grille, and propeller

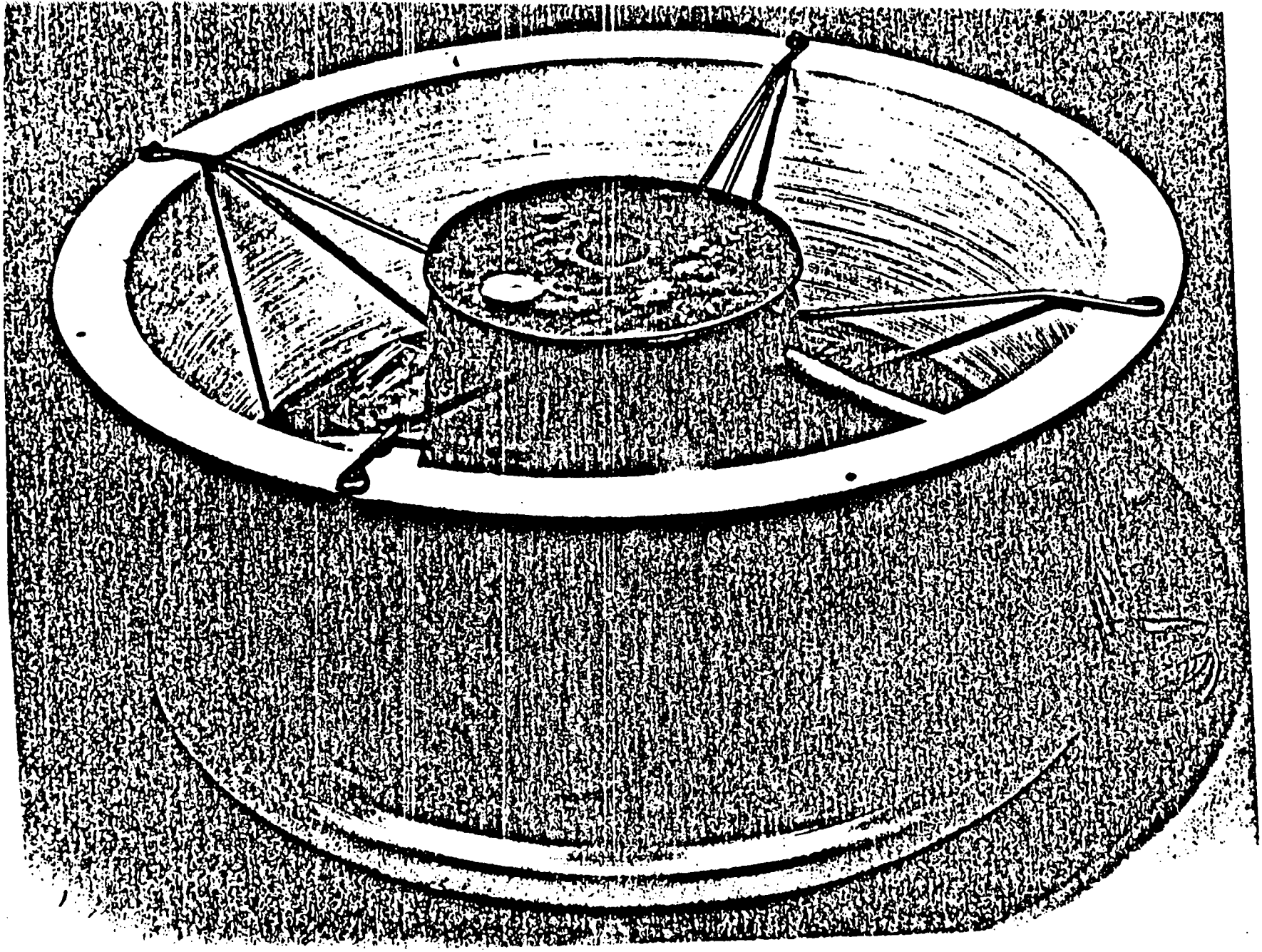

Figure 3-1. Outdoor Fan Diffuser Ring

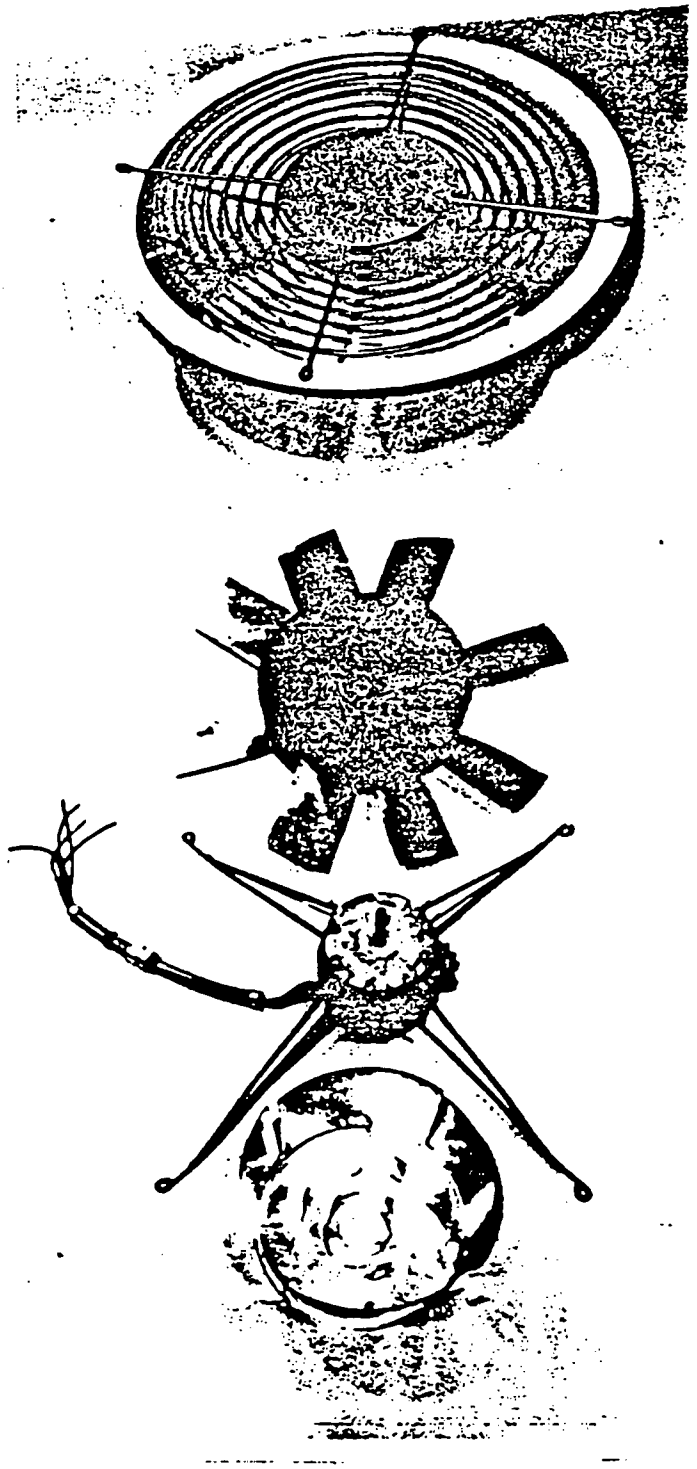

Figure 3-2. Components of the Preprototype Outdoor Fan Assembly.

assembly is estimated at $69.77. This is approximately twice the cost of the conventional outdoor air mover. The electrical energy saving potential of this air mover as applied is approximately 100 watts. The economic value of this energy taken for 6000 hours of operation per year at 5¢/kWh is approximately $30 per year. Assuming an effective retail price three times the factory cost yields a payback time of 3.5 years for the premium cost to be associated with this air mover.

In addition, it must be noted that the initial flow specification called for 2900 scfm. System optimization studies performed after preprototype hardware specifications were frozen indicate that the optimum air flow is 2600 scfm. Since air horsepower varies as the cube of the flow rate, a fan scaled to this new flow would consume 61 percent of the indicated power or about 91 watts. For a unit of nominally 3.5 tons cooling capacity, this would represent a power reduction of more than half without airfoil blades or single-speed motor.

The radiated noise from this fan does not exceed an SRN of 20. Since no noise-abating treatment has been applied to the diffuser shroud and since the grille used is more flexible than desired, a version of this air mover in prototype form should be even quieter.

SECTION 4.0

CONCLUSIONS

1. The achieved static efficiency of the preprototype outdoor air mover is approximately 50 percent.

2. The preprototype air mover consumes 150 watts of electrical power to move 3070 scfm of 47°F air through the preprototype outdoor unit which has a dry coil suction side pressure drop of 0.09 inches of water.

3. The electrical power saved relative to a replacement air mover of conventional construction is approximately 100 watts.

4. The premium first cost of the air mover should be recoverable from energy savings in less than 4 years assuming 6000 hours of operation per year, the cost of electricity at 5¢/kWh, and the effective retail cost at three times the factory cost.

5. The use of airfoil-shaped blades (untested) instead of the cambered plate blades as developed would improve static efficiency by about 5 percentage points.

6. The use of a stator vane row in combination with a diffuser stack (as tested) would improve static efficiency by about 5 percentage points.

7. Airfoil-shaped blades appear economically viable only if their incremental cost relative to cambered plate blades is negligible, as might be the case for a molded plastic fan.

8. Implementation of the stator vane row is not economically viable.

SECTION 5.0

REFERENCES

1. Veyo, S. E., "An Optimized Two-Capacity Advanced Electric Heat Pump", ASHRAE Journal, Vol. 24, No. 11, November 1982, pp. 42-49.

2. ARI Standard 270-75, "Sound Rating of Outdoor Unitary Equipment", 1975.

3. Wislicenus, G. F., Fluid Mechanics of Turbomachinery, Dover Publications, Inc., New York, 1965, pp. 32-50, 119-130, 226-259.

4. Wright, T., "A Velocity Parameter for the Correlation of Axial Fan Noise", Noise Control Engineering, Vol. 19, No. 1, July-August 1982, pp. 17-25.

5. Wright, T., "Efficiency Prediction for Axial Fans", Proceedings of the Conference on Improving Efficiency in HVAC Equipment for Residential and Small Commercial Buildings, Purdue University, October 1974, pp. 179-185.

6. Keuthe, A. M. and Schetzer, J. D., Foundations of Aerodynamics, John Wiley and Sons, Inc., New York, 1959, pp. 57-74.

7. Sovran, G. and Klomp, E. D., "Experimentally Determined Optimum Geometries for Rectilinear Diffusers with Rectangular, Conical, or Annular Cross Sections", Fluid Mechanics of Internal Flow, Elsevier Publishing Company, New York, 1969, pp. 332-371.

8. Mellor, G. L., "An Analysis of Axial Compressor Cascade Aerodynamics--Part I", Transactions of the ASME, Journal of Basic Engineering, September 1959, pp. 302-378.

9. Emergy, J. C., et. al., "Systematic Two-Dimensional Cascade Tests of NACA 65-Series Compressor Blades at Low Speed", NACA TR-1368, 1958.

10. Smith, L. H., Jr., "Casing Boundary Layers in Multistage Compressors", Flow Research on Blading, Elsevier Publishing Company, New York, 1970, pp. 275-300.

11. Koch, C. C., "Stalling Pressure Rise Capability of Axial Flow Compressor Stages", ASME Journal of Engineering for Power, Vol. 103, No. 4, October 1981, pp. 645-656.

12. Greitzer, E. M., "The Stability of Pumping Systems--The 1980 Freeman Scholar Lecture", ASME Journal of Fluids Engineering, Vol. 103, June 1981, pp. 193-242.

13. AMCA Standards, Bulletin 210, 1967.

SECTION 6.0

NOMENCLATURE

C	Blade chord, inches.
$C_{p_o}, C_{p_d}, C_{p_{TL}}$	Power coefficients, dimensionless.
D	Fan tip diameter, ft.
d	Fan hub diameter, ft.
G	Blade tip clearance gap, ft.
g	Gravitational constant, 32.16 ft/sec^2.
H	Fan total head rise, ft.
K	Blade surface velocity spiking factor, dimensionless.
K_ℓ	Loss coefficient for vane row and diffuser, dimensionless.
K_s	Span factor for tip clearance loss, dimensionless.
N	Fan speed, rpm.
PWL	Sound power level, dB re 10^{-12} watts.
ΔP_s	Static pressure rise across fan, in-H_2O.
ΔP_T	Total pressure rise across fan, $\Delta P_T = \Delta P_s + q_e$, in-$H_2O$.
Q	Volume flow rate, ft^3/min or cfm.
$\hat{Q}$	Volume flow rate, ft^3/sec.
q_e	Exit velocity pressure, in-H_2O.
R	Fan tip radius, inches.
R_h	Fan hub radius, inches.
r	Local radial position, inches.
s	Blade-to-blade circumferential separation, inches.
V_a	Axial velocity in blade row annulus, ft/sec.
V_p	Blade surface peak or maximum velocity, ft/sec.

V_T	Fan tip speed, $V_T = \pi$ N D/60, ft/sec.
W_s	Fan shaft power, hp.
x	Normalized radial position, x = r/R, dimensionless.
α_g	Blade section geometric pitch angle measured from plane of rotation to blade chord, degrees.
α_{g_R}	Value of α_g at hub or blade root, degrees.
δ_T	Normalized tip gap, δ_T = 2 G/D, dimensionless.
η_s	Static efficiency, $\eta_s = 1.576 \times 10^{-2}$ Q ΔP_s/P, percent.
η_T	Total efficiency, $\eta_T = 1.576 \times 10^{-2}$ Q ΔP_T/P, percent.
ϕ_c	Blade section circular arc camber, degrees.
ϕ	Flow coefficient, dimensionless.
Ψ_T	Total pressure coefficient, dimensionless.
ρ	Air mass density, slugs/ft^3 (lb·sec^2/ft^4).
σ	Blade solidity, σ = C/s, dimensionless.
$\overline{\sigma}$	Mean blade solidity at x = 0.75, dimensionless.
σ_T	Value of σ at the blade tip, dimensionless.
σ_h	Value of σ at the blade hub, dimensionless.